Journal Pre-proof

Monoacylglycerol lipase inhibitor JJKK048 ameliorates ABCG2 transporter-mediated regorafenib resistance induced by hypoxia in triple negative breast cancer cells

Elena Puris , Sabrina Petralla , Seppo Auriola , Heidi Kidron , Gert Fricker , Mikko Gynther

PII: S0022-3549(23)00198-3
DOI: https://doi.org/10.1016/j.xphs.2023.05.012
Reference: XPHS 3087

To appear in: *Journal of Pharmaceutical Sciences*

Received date: 1 March 2023
Revised date: 11 May 2023
Accepted date: 13 May 2023

Please cite this article as: Elena Puris , Sabrina Petralla , Seppo Auriola , Heidi Kidron , Gert Fricker , Mikko Gynther , Monoacylglycerol lipase inhibitor JJKK048 ameliorates ABCG2 transporter-mediated regorafenib resistance induced by hypoxia in triple negative breast cancer cells, *Journal of Pharmaceutical Sciences* (2023), doi: https://doi.org/10.1016/j.xphs.2023.05.012

Monoacylglycerol lipase inhibitor JJKK048 ameliorates ABCG2 transporter-mediated regorafenib resistance induced by hypoxia in triple negative breast cancer cells

Elena Puris [1], Sabrina Petralla [1], Seppo Auriola [2], Heidi Kidron [3], Gert Fricker [1] and Mikko Gynther [1, *]

[1] Institute of Pharmacy and Molecular Biotechnology, Ruprecht-Karls-University, Im Neuenheimer Feld 329, 69120 Heidelberg, Germany

[2] School of Pharmacy, University of Eastern Finland, P.O. Box 1627, 70211 Kuopio, Finland

[3] Drug Research Program, Division of Pharmaceutical Biosciences, Faculty of Pharmacy, University of Helsinki, Helsinki, Finland. Viikinkaari 5 E, P.O. Box 56, 00014, Finland

[*] Correspondence: mikko.gynther@uni-heidelberg.de

Keywords: Anti-cancer drug resistance, breast cancer resistance protein, hypoxia, monoacylglycerol lipase, triple negative breast cancer

Abstract

Triple negative breast cancer (TNBC) is among the most aggressive and deadly cancer subtypes. Intra-tumoral hypoxia is associated with aggressiveness and drug resistance in TNBC. One of the underlying mechanisms of hypoxia-induced drug resistance is the elevated expression of efflux transporters such as breast cancer resistant protein (ABCG2). In the present study, we investigated the possibility of ameliorating ABCG2-mediated drug resistance in hypoxic TNBC cells by monoacylglycerol lipase (MAGL) inhibition and the consequent downregulation of ABCG2 expression.

The effect of MAGL inhibition on ABCG2 expression, function, and efficacy of regorafenib, an ABCG2 substrate was investigated in cobalt dichloride ($CoCl_2$) induced pseudohypoxic TNBC (MDA-MB-231) cells, using quantitative targeted absolute proteomics, qRT-PCR, anti-cancer drug accumulation in the cells, cell invasiveness and resazurin-based cell viability assays.

Our results showed that hypoxia-induced ABCG2 expression led to low regorafenib intracellular concentrations, reduced the anti-invasiveness efficacy, and elevated half maximal inhibitory concentration (IC_{50}) of regorafenib *in vitro* MDA-MB-231 cells. MAGL inhibitor, JJKK048, reduced ABCG2 expression, increased regorafenib cell accumulation, which led to higher regorafenib efficacy.

In conclusion, hypoxia-induced regorafenib resistance due to ABCG2 over-expression in TNBC cells can be ameliorated by MAGL inhibition.

Introduction

Breast cancer is the most prevalent cancer type, and accounts for approximately 12 % of all diagnosed cancer cases globally [1]. Breast cancer is systematically divided into several subtypes according to the marker genes expressed by the cancerous cells and the associated clinical outcomes of the tumor type [2]. Triple negative breast cancer (TNBC), described by the lack of estrogen, progesterone, and human epidermal growth factor receptor 2 expression, is among the most aggressive and deadly cancer subtypes, with high rates of tumor recurrence and poor overall survival [3]. Recent advances in the discovery of molecular subtypes and immunological heterogeneity in TNBC, have aided the recognition of a variety of clinical phenotypes. These advances have allowed the use of targeted inhibitors and checkpoint inhibitors in TNBC treatment. However, chemotherapy remains the mainstay therapy against TNBC and still most of the patients eventually develop a drug resistance resulting in metastatic relapses of the disease [4].

Intra-tumoral hypoxia is associated with invasion, metastasis, and drug resistance in breast cancer [5,6]. Cancer cells respond to the hypoxic microenvironment through the activity of hypoxia-inducible factors 1α (HIF1A) and 2 (HIF2) [7], and the high expression of HIF1A has been associated with advanced disease and poor clinical outcome in breast cancer patients [8,9]. Thus, targeting HIF1A has been considered as a strategy for treating TNBC and other cancers with high HIF1A expression [10]. However, there are currently no HIF1A inhibitors in clinical use for the treatment of TNBC.

Upregulation of HIF1A expression leads to elevated expression of several genes reducing drug efficacy, including efflux transporters, P-glycoprotein (ABCB1) and breast cancer resistance protein (ABCG2) [11,12]. Furthermore, hypoxia mediates nuclear factor kappa B (NFκB) activation [13], which leads to an additive effect on the ABCB1 and ABCG2 expression [14,15]. The high expression of ABCB1 and ABCG2 reduces the efficacy of several anti-cancer drugs, such as irinotecan, paclitaxel, sorafenib and regorafenib, as they are actively removed out from the cancer cells by the transporter(s) resulting in subeffective intracellular concentrations [16-18]. Therefore, the reduction of efflux transporter expression and/or activity has been considered as a potential strategy to resensitize cancer cells to drug treatment [16]. Despite promising preclinical results, the development of ABCB1 and ABCG2 inhibitors for clinical use has not been successful thus far due to several reasons, including pharmacokinetic interactions, which lead to elevated anti-cancer drug concentrations in

healthy tissues [19]. Therefore, there is a demand for other strategies to overcome efflux transporter-mediated anti-cancer drug resistance.

In TNBC, high ABCG2 expression has been reported, and it can result in transporter-mediated resistance to anti-cancer drugs, which are substrates of ABCG2 [20,21]. Regorafenib is a multikinase inhibitor currently in clinical use against the hepatic, colorectal and gastric cancers [22]. In addition, recent studies suggest that regorafenib can possess a potential for the treatment of TNBC [23,24]. However, high ABCG2 expression in TNBC can result in a potential intrinsic transporter-mediated regorafenib resistance limiting its use. In addition, regorafenib reduces angiogenesis, and thus, can further induce the hypoxic tumor microenvironment during the drug treatment [25]. Consequently, the regorafenib therapy-induced hypoxia may promote the ABCG2-mediated therapy resistance. Therefore, to utilize the full potential of regorafenib against TNBC, the drug may have to be combined with a compound mitigating ABCG2-mediated drug resistance.

As it has been previously shown that hypoxia induces NFκB signaling, which takes part in the elevated ABCB1 and ABCG2 expression in cancer cells, target proteins taking part in NFκB activation can be considered as potential targets for overcoming ABCB1 and ABCG2-mediated anti-cancer drug resistance in hypoxic tumors [13-15]. The activation of NFκB signaling increases the production of proinflammatory cytokines such as tumor necrosis factor α (TNFA) and prostaglandin-endoperoxide synthase 2 (PSGT2) expression, thus having a pro-inflammatory function in cancer [15,26,27]. The induction of PSGT2 results in elevated prostaglandin E2 levels, which in turn leads to further NFκB activation through prostaglandin receptors [28]. Monoacylglycerol lipase (MAGL) is an enzyme that catalyzes the conversion of monoacylglycerides to free fatty acids and glycerol and produces arachidonic acid required for prostaglandin production mediated by PSGT2 [29]. Zhu et al. (2016) showed that MAGL upregulation in hepatocellular carcinoma cells activates NFκB signaling, and the activation can be modulated by MAGL inhibitor JZL184 [30]. MAGL has elevated expression in many types of aggressively growing cancers, including TNBC, and plays a key role in tumorigenesis and metastasis through the production of intracellular free fatty acids to fuel cancer cell proliferation and NFκB signaling [29]. Therefore, we considered it as a promising target protein for overcoming transporter-mediated drug resistance in hypoxic tumors. Furthermore, there are several well-characterized and potent MAGL inhibitors available, which have been shown to be well tolerated in animal studies [31]. These MAGL inhibitors include (1H-1,2,4-triazol-1-yl) methanone (JJKK048), an ultra-potent and selective MAGL inhibitor, which has been shown to be effective both *in vitro* and *in vivo* [32,33].

In the present study, the aim was to investigate the effect of hypoxia on ABCG2 expression in TNBC cells and the consequent association with reduced cell accumulation and anti-proliferative efficacy of ABCG2 substrate, regorafenib. Another aim of the study was to provide mechanistic evidence that MAGL inhibition can be used as a novel strategy to overcome ABCG2-mediated drug resistance induced by hypoxia in TNBC cells. To reach these aims, we investigated the effect of cobalt dichloride ($CoCl_2$) induced pseudohypoxia on the NFκB phosphorylation, mRNA, and protein expression of HIF1A, mRNA expression of PSGT2, TNFA, vascular endothelial growth factor α (VEGFA), inducible by hypoxia and NFκB signaling, as well as the protein expression of MAGL, ABCB1 and ABCG2. In addition, we measured the function of ABCG2 and the subsequent effect on cell accumulation and efficacy of regorafenib in TNBC cell line MDA-MB-231. Furthermore, we investigated whether an MAGL inhibitor, JJKK048, can resensitize cancer cells to regorafenib by reducing ABCG2 expression via inhibition of NFκB signaling.

Materials and Methods

Materials

Acetonitrile, ethylenediaminetetraacetic acid (EDTA), guanidine hydrochloride, Tris-HCl, formic acid, dithiothreitol (DTT), urea, protease inhibitor cocktail, Cobalt dichloride hexahydrate ($CoCl_2 \cdot 6H_2O$), Ko143, lucifer yellow and carbamazepine were purchased from Sigma-Aldrich (St. Louis, MO). Regorafenib and JJKK048 were purchased from MedChemExpress (Sollentuna, Sweden). ProteoExtract® Subcellular Proteome Extraction Kit was purchased from Merck KGaA (Darmstadt, Germany). The absolute quantified stable isotope-labelled peptides SpikeTides™ TQL were purchased from JPT Peptide Technologies GmbH (Berlin, Germany). Protease-Max surfactant, tosylphenylalanylchloromethyl ketone-treated trypsin, and lysyl endopeptidase (LysC) were purchased from Promega (Madison, WI, USA). BioRad DC Protein Assay was purchased from EnVision (PerkinElmer Inc., Waltham, MA, USA).

Cells

The MDA-MB-231 cells were a kind gift from Professor Stefan Wiemann at the Division of Molecular Genome Analysis, Deutsches Krebsforschungszentrum, Heidelberg, Germany. The cells were incubated in high glucose Dulbecco's modified Eagle medium (DMEM; Invitrogen, Carlsbad, CA, USA), supplemented with 10 % fetal bovine serum (FBS;

Invitrogen, Carlsbad, CA, USA) and 1 % penicillin/streptomycin at 37 °C under 5 % CO_2 in humidified incubator.

Quantitative Reverse Transcription Polymerase Chain Reaction (qRT-PCR)

Cells were seeded in 6-well plates and were allowed to attach to the plate for 24 h. Total RNA was extracted at 6 h after exposure to pre-treatments with culture medium (control), in the presence of 100 µM $CoCl_2$ and in the presence of 100 µM $CoCl_2$ and 0.5 µM JJKK048. The RNA extraction was performed with the RNeasy Mini Kit (Qiagen, Stockach, Germany) according to the manufacturer's instructions and quantified by a NanoDrop (Thermo Fisher Scientific, Dreieich, Germany). An iScript™ cDNA synthesis kit (Bio- Rad Laboratories, Munich, Germany) was used for cDNA was synthesis using 1 µg of total RNA for reverse transcription. Subsequently, the synthesized cDNA was mixed with the PowerUp SYBR Green MasterMix (Applied Biosystems, Waltham, MA, USA) and gene-specific primers (Thermo Fisher Scientific, Dreieich, Germany) shown in Table 1. The primers were designed and validated as previously described [34]. Normalized relative expression in the samples was calculated by dividing the relative quantity of a given target/sample by the geometric mean of the relative quantities of the housekeeping gene glyceraldehyde- 3- phosphate dehydrogenase (GADPH) according to Taylor et al. (2019) [35]. The qRT-PCR was performed using a LightCycler 96 (Roche Diagnostics), data was acquired using LightCycler® 96 SW 1.1 software, v. 1.1.0.1320 (Roche Diagnostics, Mannheim, Germany; 2011).

Western blot analysis

Cells were seeded on 6 well plates and were allowed to attach for 24 h. Cell pellets of untreated MDA-MB-231 cells (Control), 100 µM $CoCl_2$ treated as well as 100 µM $CoCl_2$ and 0.5 µM JJKK048 treated cells were collected after 6 h incubation. Untreated and treated MDA-MB-231 cells were lysed in RIPA buffer (150 mM NaCl, 1.0 % IGEPAL® CA-630, 0.5 % sodium deoxycholate, 0.1 % SDS, 50 mM Tris, pH 8.0; 1% protease inhibitor cocktail; Sigma-Aldrich) and total protein sample content determined by using the DC™ Protein Assay Kit (Bio-Rad) according to the manufacturer's recommendations. 15 µg of each sample with Laemli loading buffer (1 M Tris-HCl, pH 6.8; 20 % sodium dodecyl sulphate; 0.4 µl/ml glycerol; 2 g/l bromophenol blue and 2 M dithiothreitol) were resolved in 8 % acrylamide gel through SDS-PAGE and proteins transferred into nitrocellulose membranes. Membranes were then blocked in PBS-0.1 % Tween 20–5 % skimmed milk and incubated

o/n with primary antibodies against HIF1A (1:1000; rabbit polyclonal Cat# sc-10790, SantaCruz Biotechnology; kindly provided by Prof. Barbara Monti, Department of Pharmacy and Biotechnology, University of Bologna, Italy) and GAPDH (1:5000; rabbit polyclonal Cat# NB300-327, Novusbio). After washes, membranes were incubated with HRP-linked secondary antibody goat anti-rabbit (1:5000; Cat# 111-035-144, Jackson ImmunoResearch Labs) and visualized by Western Lightning Plus- ECL (Enhanced ChemiLuminescence Substrate; PerkinElmer). Images were acquired with a Bio-Rad Chemidoc imager and densitometric analysis was performed by using Bio-Rad Image Lab software (Version 5.1).

NFκB p65 phosphorylation analysis

Cells seeded in 96-well plates were allowed to attach to the plate for 24 h. The cells were lysed and collected 6 h after exposure to pre-treatments with culture medium (control), in the presence of 100 µM $CoCl_2$ and in the presence of 100 µM $CoCl_2$ and 0.5 µM JJKK048. A commercial NFκB p65 (Total/Phospho) Human InstantOne™ ELISA Kit Catalog # 85-86083-11 (Invitrogen, Carlsbad, CA, USA) was used to measure the phosphorylated and total NFκB p65 expression in the cell lysates.

Liquid Chromatography Mass Spectrometry (LC−MS/MS) methods

The high-pressure liquid chromatography equipment consisted of a Waters 2695 pump, Waters autosampler, and column oven (Waters, Milford, MA, USA). For liquid chromatography a C18 reverse phase PerfectSil Target ODS-3 HD (100 mm × 2.1 mm, 3 µm) column (MZ-Analysentechnik GmbH, Mainz, Germany) was used. The MS analysis of regorafenib and JJKK048 was performed with Waters Micromass Quattro Ultra Pt mass spectrometer (Waters, Milford, MA, USA) equipped with an electrospray ionization source. Analyte detection was performed using multiple reaction monitoring, the transitions being 483 → 288, 435 → 366 and 237 → 194 for regorafenib, JJKK048 and carbamazepine, respectively. Mass Lynx V4.1 software was used for data acquisition and processing. The lower limit of quantification for regorafenib and JJKK048 were 20 nM and 50 nM, respectively. Linearities of the calibration curves were evaluated by regression analysis. The method was selective, accurate, and precise over the calibration range. The accuracies and precisions for quality control concentrations of 20 % were considered acceptable.

Quantitative targeted absolute proteomic (QTAP) analysis

The absolute protein concentration of ABCB1 and ABCG2, membrane bound enzyme MAGL, and plasma membrane marker Na^+/K^+-ATPase were measured in the crude membrane fraction of untreated MDA-MB-231 cells (control), 100 µM $CoCl_2$ treated as well as 100 µM $CoCl_2$ and 0.5 µM JJKK048 treated cells. The treatments were added 48 h prior to collecting the cells for crude membrane fraction isolation using ProteoExtract Subcellular Proteome Extraction Kit (Merck KGaA, Darmstadt, Germany). Bio-Rad DC Protein Assay was used for the measurement of total protein concentrations in the isolated MDA-MB-231 cell crude membrane fractions. After that, the samples were prepared as previously described [36,37].

For the LC-MS/MS analysis, an Agilent 1290 Infinity LC (Agilent Technologies, Waldbronn, Germany) system coupled to an Agilent 6495 Triple Quadrupole Mass Spectrometer equipped with an ESI source (Agilent Technologies, Palo Alto, CA, USA), and for the HPLC an Advance Bio Peptide Map column (2.1 × 250 mm; 2.7 µm) was used [37]. Agilent MassHunter Workstation Acquisition software (Agilent Technologies, Data Acquisition for Triple Quad., version B.03.01) was used for acquiring the data, after which the data was processed using Skyline software (version 4.1). The MRM transitions used for the quantification are presented in Table 2. The lower limit of quantification was determined as previously described [38].

Vesicle preparation

Crude membrane vesicles were prepared as described [39]. Sf9 cells were grown at 27 °C as a suspension culture in HyClone SfX Insect cell medium (Thermo Fisher Scientific, Waltham, MA, USA) with 5 % FBS (Gibco, Invitrogen, NY, USA). For expression of human BCRP, the cells were infected with recombinant baculovirus carrying the BCRP gene and harvested by centrifugation at 1000 g for 10 min (+4 °C) 60 h after infection and washed once with phosphate buffered saline. The harvested cells were washed twice with buffer containing 50 mM Tris-HCl (pH 7.0) and 300 mM mannitol and then homogenized in membrane buffer (50 mM Tris-HCl (pH 7.0), 50 mM mannitol and 2 mM EDTA) using a Dounce homogenizer (pestle B) for 40 strokes. The cell lysate was centrifuged at 800 g for 10 min the supernatant was further centrifuged at 100, 000 g for 75 min at + 4°C to pellet the membrane. The membrane pellet was resuspended in membrane buffer and passed 20 times through a 27-gauge needle to form vesicles. Cholesterol was loaded to the vesicles by incubation for 20 min on ice with 2.5 mM cholesterol in complex with randomly methylated-β-cyclodextrin

(Cyclolab, Hungary), whereafter the vesicles were collected by centrifugation at 100,000 g for 75 min and resuspended in membrane buffer. The protein concentration of the vesicle preparation was measured with the Bio-Rad protein assay based on the Bradford method (Bio-Rad Laboratories Inc., Hercules, CA, USA) and aliquots of membrane vesicles were flash frozen in liquid nitrogen and stored at -80 °C.

Vesicular transport assay

Vesicular transport experiments were performed according to the previously described protocol [40], using the rapid filtration technique with MultiscreenHTS96-well, 1.0/0.65 µm pore, glass fiber filter plates (MSFBN6B50) Millipore (Molsheim, France) on a MultiScreenHTS vacuum manifold (Millipore). Briefly, Sf9 transport assays for ABCG2 substrate lucifer yellow were conducted by pre-incubating vesicles (50 µg of total protein) either with lucifer yellow alone or lucifer yellow with BCRP inhibitor Ko143 (1 µM) in buffer (40 mM MOPS-Tris (pH 7.0), 60 mM KCl and 6 mM $MgCl_2$) for five min. This step followed by adding either prewarmed Mg-ATP or plain buffer (control) to achieve a final concentration of lucifer yellow 50 µM. The ice-cold washing mix (40 mM MOPS-Tris (pH 7.0) and 70 mM KCl) was used to terminate the reactions after 10 min incubation. The samples were immediately filtered by the rapid filtration technique using MultiscreenHTS96-well, 1.0/0.65 µm pore, glass fiber filter plates (MSFBN6B50) Millipore (Molsheim, France) on a vacuum manifold (Millipore, Molsheim, France). The filters were washed with washing mix five times followed by complete drying. After that, 100 µl 0.1 M NaOH were added to the filter plate to elute the lucifer yellow samples, which were subsequently neutralized with an equal amount of 0.1 M HCl. For analysis, lucifer yellow samples were eluted with 100 µl 0.1 M NaOH and neutralized with an equal amount of 0.1 M HCl. The lucifer yellow fluorescence were quantified by TECAN infinite F200 Pro plate reader (Männedorf, Switzerland) using excitation and emission wave lengths of 465 and 590 nm, respectively.

The Sf9 transport experiments for regorafenib was conducted with minor modifications. Sf9 vesicles (50 µg of total protein) were pre-incubated with either regorafenib alone or in combination with Ko143 (1 µM) in buffer (40 mM MOPS-Tris (pH 7.0), 60 mM KCl and 6 mM $MgCl_2$) for five min. After that, prewarmed Mg-ATP or plain buffer (control) were added to achieve a final concentration of regorafenib 0.5 µM followed by termination of the reactions by adding the ice-cold washing mix (40 mM MOPS-Tris (pH 7.0) and 70 mM KCl) after 40 min incubation. The samples were immediately filtered by the rapid filtration

technique using MultiscreenHTS96-well, 1.0/0.65 µm pore, glass fiber filter plates (MSFBN6B50) Millipore (Molsheim, France) on a vacuum manifold (Millipore, Molsheim, France). The filters were washed with washing mix five times followed by complete drying. Finally, 100 µl of 50 % methanol containing internal standard carbamazepine were added to the filter plate to elute regorafenib. The samples were analyzed using LC-MS/MS.

Drug cell accumulation analysis

The cell accumulation of JJKK048, lucifer yellow and regorafenib was investigated in MDA-MB-231 cells. The cells were seeded onto 48-well plates, after which the cells were allowed to attach on the plates for 24 h, followed by pre-treatment by the replacement of the growth medium with fresh DMEM, DMEM containing 100 µM $CoCl_2$ or 100 µM $CoCl_2$ and 0.5 µM JJKK048. After 48 h incubation, the cells were washed twice with 300 µl of 37 °C DPBS, followed by addition of either 300 µl of 0.5 µM JJKK048, 100 µM lucifer yellow or 2.5 µM regorafenib (with or without 1 µM Ko143) dissolved in 37 °C DPBS. In addition, in the ABCG2 inhibition experiments, 1 µM Ko143 was added to the cells 30 min before washing the cells. The cells were incubated at 37 °C for 20 min. Subsequently, the cells were washed with DPBS and lysed either with 100 µl of ACN containing internal standard (JJKK048 and regorafenib) or 100 µl of 0.1 M NaOH (lucifer yellow). To measure total protein concentration, cells in three wells subjected to each pre-treatment were lysed with 100 µl of 0.1 M NaOH. The protein concentrations were determined by Bio-Rad Protein Assay (EnVision, PerkinElmer, Inc., Waltham, MA, USA). Each experiment was conducted in triplicate and repeated three times.

Cell invasion assay

For the cell invasion assay Thincert 24 well-plate and filter inserts (Greiner Bio-one, Frickenhausen, Germany) with 8 µm pore size were used. After coating the filters with 30 µg of Matrigel®, 25 000 cells were seeded in 200 µl of FBS free medium on the filters and 600 µl of DMEM containing 10 % FBS as chemoattractant was inserted in the wells. For inducing pseudohypoxia, 100 µM $CoCl_2$ was added in both filter inserts and the wells. The cells were allowed to pass through the Matrigel covered filters for 20 hours. The non-invasive cells were removed from the filters using a cotton swab, after which the invasive cells were fixed with methanol and stained with 0.1 % crystal violet. The cells were then counted under the microscope using 10 × magnification. Three randomly selected fields were used for the cell

counting from each sample. The experiment was repeated three times. The pseudohypoxia effect on MDA-MB-231 cell invasiveness was determined by comparing untreated cells (control) and 100 µM $CoCl_2$ treated cells. The effect of pseudohypoxia on regorafenib's ability to reduce cell invasiveness was investigated by treating the cells with 0.25 µM regorafenib alone, in combination with 100 µM $CoCl_2$ and, in the presence of 100 µM $CoCl_2$ and 0.5 µM JJKK048. The effect of JJKK048 on pseudohypoxic cell invasiveness was investigated by treating the cells with 100 µM $CoCl_2$ in combination with 0.5 µM JJKK048. The used regorafenib and JJKK048 concentrations were selected to be below concentrations which affected cell viability.

Cell viability analysis

Cells were seeded in 96-well plates and were allowed to attach to the plate for 24 h. To establish a suitable $CoCl_2$ concentration for the induction of pseudohypoxia, the cells were treated with $CoCl_2$ for 72 hours. To determine the half-maximal inhibitory concentration (IC_{50}) of JJKK048, the cells were with and without 100 µM $CoCl_2$. The IC_{50} value of regorafenib was investigated without $CoCl_2$ and JJKK048 (control), in the presence of 100 µM $CoCl_2$ and in the presence of 100 µM $CoCl_2$ and 0.5 µM JJKK048. Cell viability was analyzed by PrestoBlue Assay Kit (Invitrogen, Carlsbad, CA, USA). Each experiment was conducted in triplicate and repeated three times.

Statistical analysis

The present study is an exploratory study, and the samples size of the study was based on the previous in vitro QTAP and mRNA expression studies. The data are presented as mean ± standard deviation (SD) (n=3-4) for the gene expression, Western blot, QTAP analysis, JJKK048, regorafenib cell accumulation, regorafenib IC_{50} levels and the cell invasiveness results. Statistical significance of changes between the groups was evaluated by One-way ANOVA followed by Tukey's multiple comparisons test. A *p*-value less than 0.05 was considered statistically significant. GraphPad Prism, version 5.03 (GraphPad Software, San Diego, CA) was used for the statistical analysis.

Results

NFκB activated by pseudohypoxia in MDA-MB-231 cells can be reduced by MAGL inhibition

To determine the $CoCl_2$ concentration used for producing chemically induced hypoxia (pseudohypoxia) in the MDA-MB-231 cells, we treated the cells for 72 h with $CoCl_2$ and measured the viability (Fig. 1 A). The $CoCl_2$ IC_{50} value was 265 µM. For the induction of pseudohypoxia in the cells, we selected 100 µM $CoCl_2$ as the cell viability was not significantly reduced at that concentration. Next, we investigated whether the 100 µM $CoCl_2$ was able to induce hypoxia-like effects and NFκB signaling in the cells. $CoCl_2$ treatment significantly increased the mRNA and protein expression of HIF1A (Fig. 1 B and C). The HIF1A gene expression was 20-fold higher, while the protein expression increased 3-fold in the pseudohypoxic cells compared to the normoxic control cells. The phosphorylated to total NFκB p65 expression ratio was 1.4-fold higher in the 100 µM $CoCl_2$ treated cells compared to the normoxic control cells (Fig. 2 B). Moreover, the results showed a statistically significant 8-fold, 2.5-fold and 46-fold increase in the mRNA expression of NFκB downstream genes VEGFA, PTGS2 and TNFA, respectively (Fig. 2 B).

To investigate the effect of the MAGL inhibition on $CoCl_2$ induced pseudohypoxia and NFκB signaling, we treated the MDA-MB-231 cells with 0.5 µM JJKK048 together with 100 µM $CoCl_2$ and measured the expression of hypoxia and NFκB signaling markers (Fig. 1 and 2). JJKK048 was able to significantly decrease the mRNA expression of VEGFA, PTGS2 and TNFA in pseudohypoxic cells, as compared to the $CoCl_2$ treated cells (Fig. 2 B): the mRNA expression of VEGFA, PTGS2 and TNFA were reduced by 2.5-fold, 1.7-fold, and 37-fold, respectively. In addition, JJKK048 treatment in pseudohypoxic cells resulted in a 2-fold reduction of phosphorylated to total NFκB p65 expression ratio compared to the $CoCl_2$ treated cells (Fig. 2 A). On the contrary, JJKK048 did not have a significant effect on HIF1A protein and gene expression (Fig. 1 B and C).

MAGL inhibitor JJKK048 is readily accumulated intracellularly and reduces MDA-MB-231 cell viability

The protein expression of MAGL was investigated in the MDA-MB-231 cells using QTAP analysis. The results showed robust MAGL protein expression (Fig. 3 A). The increase in MAGL protein levels after $CoCl_2$ treatment was not statistically significant (p = 0.065). However, the MAGL protein expression was statistically significantly reduced (2.3-fold) due to JJKK048 treatment as compared to the $CoCl_2$ treated cells (Fig. 3 A). JJKK048 effect on MDA-MB-231 cell viability was similar in both normoxic control and $CoCl_2$ treated cells with IC_{50} values of 61 µM (Fig. 3 B). For further studies with JJKK048, we selected the

concentration of 0.5 µM, as at that concentration the compound did not significantly reduce cell viability. The compound readily accumulated into both normoxic control and $CoCl_2$ treated cells when incubated with 0.5 µM of JJKK048 for 20 min (Fig. 3 C).

ABCG2 expression and function are elevated in pseudohypoxic MDA-MB-231 cells

The effect of pseudohypoxia on ABCG2 protein expression in MDA-MB-231 cells was investigated by incubating the cells for 48 h in the presence of 100 µM $CoCl_2$, followed by the QTAP analysis. The ABCG2 gene expression was measured after 6 h $CoCl_2$ incubation in MDA-MB-231 cells. Both mRNA and protein expressions were significantly increased compared to control normoxic cells (Fig. 4 A). The increase in ABCG2 mRNA and protein expressions were 4.6-fold and 3.3-fold higher in the pseudohypoxic cells compared to the control normoxic cells, respectively. Furthermore, the 48-h $CoCl_2$ treatment increased ABCG2 function leading to reduced accumulation of lucifer yellow and regorafenib in MDA-MB-231 cells (Fig. 4 B). Lucifer yellow and regorafenib were confirmed to be ABCG2 substrates by using the vesicular transport assay. Both compounds were efficiently accumulated in the ABCG2 expressing vesicles and the accumulation was significantly reduced by ABCG2 inhibitor, Ko143 (Fig 5).

ABCB1 gene and protein expressions were quantified in the control normoxic and the $CoCl_2$ treated cells. Neither ABCB1 gene expression nor protein abundance (LLOQ 0.1 fmol/µg protein) were detected in the investigated MDA-MB-231 cells.

MAGL inhibition reduces ABCG2 expression and function leading to increased cell accumulation and efficacy of regorafenib in pseudohypoxic MDA-MB-231 cells

Increases in the ABCG2 gene and protein expression-mediated by pseudohypoxia via NFκB signaling were reversed by the inhibition of MAGL by 0.5 µM JJKK048 treatment (Fig. 4 A). The decreased ABCG2 expression led to reduced activity of the transporter as the cell accumulation of ABCG2 substrates lucifer yellow and regorafenib was significantly increased in the JJKK048-treated cells compared to the cells treated with $CoCl_2$ alone (Fig. 4 B). Lucifer yellow and regorafenib cell accumulations were 2.8 and 1.4-fold higher in the pseudohypoxic JJKK048-treated cells compared to the pseudohypoxic cells without MAGL inhibition, respectively. Co-incubation of lucifer yellow and regorafenib with an ABCG2 inhibitor, Ko143, significantly increased the compounds' accumulation in pseudohypoxic cells by 2.0 and 1.2-fold, respectively (Fig. 4 B).

Finally, we investigated the effect of altered regorafenib cell accumulation on MDA-MB-231 cell invasiveness and viability. Regorafenib at 0.25 µM concentration significantly decreased the invasiveness of MDA-MB-231 cells (Fig 6 A). $CoCl_2$ treatment did not significantly increase the invasiveness of MDA-MB-231 cells, while the pseudohypoxia significantly decreased the anti-invasive effect of regorafenib as compared to normoxic conditions (p = 0.0015) (Fig. 6 A). In addition, there was no statistically significant difference in the invasiveness between the cells treated alone with $CoCl_2$ and the cells treated in combination of $CoCl_2$ and regorafenib. MAGL inhibitor, JJKK048, did not affect the cell invasiveness under pseudohypoxic conditions. However, JJKK048 was able to reverse the $CoCl_2$-mediated decrease in regorafenib anti-invasive efficacy as the number of invasive cells after the combination treatment was significantly lower compared to $CoCl_2$ treatment alone (p = 0.001) as well as to the $CoCl_2$ and regorafenib treated cells (p = 0.012) (Fig. 6 A). The IC_{50} value of regorafenib was 1.4-fold higher in $CoCl_2$ treated cells compared to normoxic control cells (p = 0.023), whereas the regorafenib IC_{50} value was 2.2-fold lower in JJKK048 and $CoCl_2$ treated cells compared to the cells treated with $CoCl_2$ alone (p = 0.01) (Fig. 6 B).

Discussion

Despite recent advances in drug development, there is still a large unmet need for efficient drug therapies against TNBC [41,42]. One significant hurdle hindering drug efficacy in TNBC is the high expression of efflux transporters such as ABCG2, which can limit drug accumulation in the target cells [42,43]. Regorafenib is a multi-kinase inhibitor, which has been shown to be a selective substrate of ABCG2 over ABCB1 [17]. In addition, regorafenib shows promise for the treatment of TNBC [23,24]. Furthermore, as regorafenib inhibits angiogenesis, it is reported to further intratumoral hypoxia, which in turn can result in acquired therapy resistance [25]. In the context of potential use of regorafenib for the treatment of TNBC, the possible hypoxia-induced resistance mechanisms, such as elevated ABCG2 expression should be considered. Therefore, in the present study, we investigated whether MAGL inhibitor JJKK048 can ameliorate ABCG2-mediated regorafenib resistance induced by hypoxia in TNBC cells.

To induce hypoxia-like changes in the MDA-MB-231 TNBC cell line, we used a $CoCl_2$ induced chemical hypoxia model. $CoCl_2$ induced pseudohypoxia generates several hypoxia-mimicking changes, including the stabilization of HIF1A, induction of HIF1A gene expression leading to induction of transcriptional factors [44]. The $CoCl_2$ induced hypoxia model is the most frequently used and well-characterized pseudohypoxia model with several

similarities to actual hypoxia in the biochemical pathways that are affected [44]. Similarly to low level of oxygen, $CoCl_2$ inhibits prolyl-hydroxylases leading to the consequent stabilization HIF1A and activation of NFκB signaling [45]. The activation of NFκB signaling is known to increase ABCG2 expression and confer anti-cancer drug resistance in breast cancer [15]. These properties make the $CoCl_2$ induced pseudohypoxia model relevant for the investigation of means to overcome hypoxia-induced and transporter-mediated drug resistance. Importantly, the model has advantages over the use of hypoxia chamber as the HIF1A stabilization remains constant during the experiments even though the cells are exposed to normal oxygen levels. We first investigated the IC_{50} value of $CoCl_2$ and the induction of HIF1A-mediated transcriptional effects in MDA-MB-231 cells. Our results show that at 100 µM concentration $CoCl_2$ did not significantly alter MDA-MB-231 viability during 72 h incubation. However, the treatment with $CoCl_2$ induced hypoxia-like changes as the mRNA and protein levels of HIF1A, and VEGFA mRNA expression were significantly increased. Hypoxia-induced elevated expression of these genes has been shown in biopsies collected from TNBC patients indicating the relevance of $CoCl_2$ induced pseudohypoxia model to mimic hypoxia in tumors [46-48]. The pseudohypoxia had an increasing effect on phosphorylated to total NFκB p65 expression ratio as well as on NFκB inducible genes, PTGS2 and TNFA. In addition, it has been shown that VEGFA expression is also inducible by NFκB activation [49].

To elucidate the effects of MAGL inhibition in pseudohypoxic TNBC cells, we used an ultrapotent and selective MAGL inhibitor, JJKK048, at a 0.5 µM concentration. The JJKK048 concentration (0.5 µM) used in the present study was selected based on the cell viability results after treating normoxic control cells and $CoCl_2$ treated cells for 72 h. At 0.5 µM the compound did not significantly alter the cell viability, although the cell uptake results indicate that the drug concentration in the cells was high enough for MAGL inhibition as the JJKK048 IC_{50} value *in vitro* against human MAGL was reported to be 363 nM [33]. Interestingly, JJKK048 reduced HIF1A mRNA but did not affect the protein expression. This is likely due to JJKK048's ability to inhibit NFκB activation, which reduces HIF1A gene expression. The HIF1A protein expression is not reduced as $CoCl_2$ stabilizes the protein. The MAGL inhibitor significantly reduced the gene expression of NFκB -inducible VEGFA, PTGS2 and TNFA genes, which were elevated in pseudohypoxic conditions, as well as phosphorylated to total NFκB p65 expression, providing evidence that MAGL inhibition can reduce NFκB signaling in hypoxic TNBC cells. As NFκB signaling induces ABCG2

expression, MAGL inhibition has the potential to prevent ABCG2 over expression in hypoxic cancer cells.

In terms of the aim to overcome transporter-mediated drug resistance in TNBC, the most remarkable result was the significant reduction of ABCG2 gene and protein expression in pseudohypoxic cells treated with 0.5 µM of the MAGL inhibitor, JJKK048, for 48 h. The decreased ABCG2 expression resulted in increased cell accumulation of the ABCG2 substrates, lucifer yellow and regorafenib [50,51]. Similar increase in cell accumulation of the compounds were observed in the presence of a selective ABCG2 inhibitor, Ko143. These findings support the notion that the changes in the lucifer yellow and regorafenib cell accumulation after different treatments are the result of altered ABCG2 expression and function. In the present study, the role of ABCB1 in the efflux of regorafenib in MDA-MB-231 cells was likely negligible, as the cell accumulation of regorafenib was increased by a selective ABCG2 inhibitor, and the ABCB1 gene and protein expression was not detected in the used cells.

In addition to the cell accumulation of regorafenib, the elevated ABCG2 expression and function in the pseudohypoxic MDA-MB-231 cells led to reduced anti-proliferative and anti-invasive efficacy of the drug. Interestingly, the $CoCl_2$-mediated reduction of regorafenib's anti-invasive effect was reversed by the MAGL inhibitor. The effect of JJKK048 alone on the invasiveness was insignificant, thus, attributing the increased regorafenib anti-invasive effect to elevated regorafenib cell accumulation. Similarly, the significantly elevated IC_{50} value of regorafenib in the $CoCl_2$ treated MDA-MB-231 cells was reversed in the presence of the MAGL inhibitor, JJKK048. This was in accordance with the elevated regorafenib cell accumulation in $CoCl_2$ and JJKK048 treated MDA-MB-231 cells compared to the $CoCl_2$ - treated cells. The results show a robust connection between ABCG2 expression, regorafenib cell accumulation, and efficacy in the used TNBC cells. However, caution should be used in generalizing the results as the study was made in one cell line. Furthermore, the present exploratory *in vitro* study is mechanistic and provides preliminary evidence in terms of clinical usability of the MAGL inhibition approach to combat ABCG2-mediated anti-cancer drug resistance. In addition, other hypoxia-inducible resistance mechanisms, which may be reversible by MAGL inhibition cannot be ruled out. Hypoxia and NFκB activation increase the expression of anti-apoptotic genes such as apoptosis regulator Bcl-2 and survivin, as well as decrease the apoptotic gene, apoptosis regulator BAX in cancer cells, which can confer regorafenib resistance [52]. Thus, the MAGL inhibition-mediated reduction of NFκB signaling

and the potentially resulting higher apoptosis susceptibility may take part in overcoming the hypoxia-induced regorafenib resistance in the MDA-MB-231 cells.

Conclusions

In conclusion, the present study showed that MAGL is expressed in MDA-MB-231 cells, and it takes part in hypoxia-activated increase in NFκB signaling. In addition, it was shown that pseudohypoxia induced ABCG2 expression and function led to ABCG2 substrate, regorafenib resistance. Importantly, an MAGL inhibitor JJKK048, ameliorated ABCG2-mediated regorafenib resistance by inhibiting NFκB signaling and reducing ABCG2 expression. The study demonstrated for the first time that MAGL inhibition can be a promising strategy to reverse ABCG2-mediated drug resistance in TNBC.

References

1. Sung H, Ferlay J, Siegel RL, Laversanne M, Soerjomataram I, Jemal A, Bray F 2021. Global Cancer Statistics 2020: GLOBOCAN Estimates of Incidence and Mortality Worldwide for 36 Cancers in 185 Countries. CA Cancer J Clin 71(3):209-249.
2. Lukasiewicz S, Czeczelewski M, Forma A, Baj J, Sitarz R, Stanislawek A 2021. Breast Cancer-Epidemiology, Risk Factors, Classification, Prognostic Markers, and Current Treatment Strategies-An Updated Review. Cancers (Basel) 13(17).
3. Garrido-Castro AC, Lin NU, Polyak K 2019. Insights into Molecular Classifications of Triple-Negative Breast Cancer: Improving Patient Selection for Treatment. Cancer Discov 9(2):176-198.
4. Yin L, Duan JJ, Bian XW, Yu SC 2020. Triple-negative breast cancer molecular subtyping and treatment progress. Breast Cancer Res 22(1):61.
5. de Heer EC, Jalving M, Harris AL 2020. HIFs, angiogenesis, and metabolism: elusive enemies in breast cancer. J Clin Invest 130(10):5074-5087.
6. Wong CC, Gilkes DM, Zhang H, Chen J, Wei H, Chaturvedi P, Fraley SI, Wong CM, Khoo US, Ng IO, Wirtz D, Semenza GL 2011. Hypoxia-inducible factor 1 is a master regulator of breast cancer metastatic niche formation. Proc Natl Acad Sci U S A 108(39):16369-16374.
7. Ye IC, Fertig EJ, DiGiacomo JW, Considine M, Godet I, Gilkes DM 2018. Molecular Portrait of Hypoxia in Breast Cancer: A Prognostic Signature and Novel HIF-Regulated Genes. Mol Cancer Res 16(12):1889-1901.
8. Generali D, Berruti A, Brizzi MP, Campo L, Bonardi S, Wigfield S, Bersiga A, Allevi G, Milani M, Aguggini S, Gandolfi V, Dogliotti L, Bottini A, Harris AL, Fox SB 2006. Hypoxia-inducible factor-1alpha expression predicts a poor response to primary chemoendocrine therapy and disease-free survival in primary human breast cancer. Clin Cancer Res 12(15):4562-4568.
9. Trastour C, Benizri E, Ettore F, Ramaioli A, Chamorey E, Pouyssegur J, Berra E 2007. HIF-1alpha and CA IX staining in invasive breast carcinomas: prognosis and treatment outcome. Int J Cancer 120(7):1451-1458.
10. Soni S, Padwad YS 2017. HIF-1 in cancer therapy: two decade long story of a transcription factor. Acta Oncol 56(4):503-515.
11. He X, Wang J, Wei W, Shi M, Xin B, Zhang T, Shen X 2016. Hypoxia regulates ABCG2 activity through the activivation of ERK1/2/HIF-1alpha and contributes to chemoresistance in pancreatic cancer cells. Cancer Biol Ther 17(2):188-198.

12. Doublier S, Belisario DC, Polimeni M, Annaratone L, Riganti C, Allia E, Ghigo D, Bosia A, Sapino A 2012. HIF-1 activation induces doxorubicin resistance in MCF7 3-D spheroids via P-glycoprotein expression: a potential model of the chemo-resistance of invasive micropapillary carcinoma of the breast. BMC Cancer 12:4.
13. Lluis JM, Buricchi F, Chiarugi P, Morales A, Fernandez-Checa JC 2007. Dual role of mitochondrial reactive oxygen species in hypoxia signaling: activation of nuclear factor-{kappa}B via c-SRC and oxidant-dependent cell death. Cancer Res 67(15):7368-7377.
14. Bentires-Alj M, Barbu V, Fillet M, Chariot A, Relic B, Jacobs N, Gielen J, Merville MP, Bours V 2003. NF-kappaB transcription factor induces drug resistance through MDR1 expression in cancer cells. Oncogene 22(1):90-97.
15. Wang W, Nag SA, Zhang R 2015. Targeting the NFkappaB signaling pathways for breast cancer prevention and therapy. Curr Med Chem 22(2):264-289.
16. Robey RW, Pluchino KM, Hall MD, Fojo AT, Bates SE, Gottesman MM 2018. Revisiting the role of ABC transporters in multidrug-resistant cancer. Nat Rev Cancer 18(7):452-464.
17. Neul C, Schaeffeler E, Sparreboom A, Laufer S, Schwab M, Nies AT 2016. Impact of Membrane Drug Transporters on Resistance to Small-Molecule Tyrosine Kinase Inhibitors. Trends Pharmacol Sci 37(11):904-932.
18. Allen JD, Brinkhuis RF, van Deemter L, Wijnholds J, Schinkel AH 2000. Extensive contribution of the multidrug transporters P-glycoprotein and Mrp1 to basal drug resistance. Cancer Res 60(20):5761-5766.
19. Callaghan R, Luk F, Bebawy M 2014. Inhibition of the multidrug resistance P-glycoprotein: time for a change of strategy? Drug Metab Dispos 42(4):623-631.
20. Uruena C, Sandoval TA, Lasso P, Tawil M, Barreto A, Torregrosa L, Fiorentino S 2020. Evaluation of chemotherapy and P2Et extract combination in ex-vivo derived tumor mammospheres from breast cancer patients. Sci Rep 10(1):19639.
21. Natarajan K, Xie Y, Baer MR, Ross DD 2012. Role of breast cancer resistance protein (BCRP/ABCG2) in cancer drug resistance. Biochem Pharmacol 83(8):1084-1103.
22. Grothey A, Blay JY, Pavlakis N, Yoshino T, Bruix J 2020. Evolving role of regorafenib for the treatment of advanced cancers. Cancer Treat Rev 86:101993.
23. Su JC, Mar AC, Wu SH, Tai WT, Chu PY, Wu CY, Tseng LM, Lee TC, Chen KF, Liu CY, Chiu HC, Shiau CW 2016. Disrupting VEGF-A paracrine and autocrine loops by targeting SHP-1 suppresses triple negative breast cancer metastasis. Sci Rep 6:28888.
24. Mehta M, Griffith J, Panneerselvam J, Babu A, Mani J, Herman T, Ramesh R, Munshi A 2021. Regorafenib sensitizes human breast cancer cells to radiation by inhibiting multiple kinases and inducing DNA damage. Int J Radiat Biol 97(8):1109-1120.
25. Juengpanich S, Topatana W, Lu C, Staiculescu D, Li S, Cao J, Lin J, Hu J, Chen M, Chen J, Cai X 2020. Role of cellular, molecular and tumor microenvironment in hepatocellular carcinoma: Possible targets and future directions in the regorafenib era. Int J Cancer 147(7):1778-1792.
26. Zheng HC 2017. The molecular mechanisms of chemoresistance in cancers. Oncotarget 8(35):59950-59964.
27. Lim JW, Kim H, Kim KH 2001. Nuclear factor-kappaB regulates cyclooxygenase-2 expression and cell proliferation in human gastric cancer cells. Lab Invest 81(3):349-360.
28. Poligone B, Baldwin AS 2001. Positive and negative regulation of NF-kappaB by COX-2: roles of different prostaglandins. J Biol Chem 276(42):38658-38664.
29. Nomura DK, Long JZ, Niessen S, Hoover HS, Ng SW, Cravatt BF 2010. Monoacylglycerol lipase regulates a fatty acid network that promotes cancer pathogenesis. Cell 140(1):49-61.
30. Zhu W, Zhao Y, Zhou J, Wang X, Pan Q, Zhang N, Wang L, Wang M, Zhan D, Liu Z, He X, Ma D, Liu S, Wang L 2016. Monoacylglycerol lipase promotes progression of hepatocellular carcinoma via NF-kappaB-mediated epithelial-mesenchymal transition. J Hematol Oncol 9(1):127.

31. Deng H, Li W 2020. Monoacylglycerol lipase inhibitors: modulators for lipid metabolism in cancer malignancy, neurological and metabolic disorders. Acta Pharm Sin B 10(4):582-602.
32. Aaltonen N, Kedzierska E, Orzelska-Gorka J, Lehtonen M, Navia-Paldanius D, Jakupovic H, Savinainen JR, Nevalainen T, Laitinen JT, Parkkari T, Gynther M 2016. In Vivo Characterization of the Ultrapotent Monoacylglycerol Lipase Inhibitor {4-[bis-(benzo[d][1,3]dioxol-5-yl)methyl]-piperidin-1-yl}(1H-1,2,4-triazol-1-yl)m ethanone (JJKK-048). J Pharmacol Exp Ther 359(1):62-72.
33. Aaltonen N, Savinainen JR, Ribas CR, Ronkko J, Kuusisto A, Korhonen J, Navia-Paldanius D, Hayrinen J, Takabe P, Kasnanen H, Pantsar T, Laitinen T, Lehtonen M, Pasonen-Seppanen S, Poso A, Nevalainen T, Laitinen JT 2013. Piperazine and piperidine triazole ureas as ultrapotent and highly selective inhibitors of monoacylglycerol lipase. Chem Biol 20(3):379-390.
34. Gynther M, Estrada ML, Loppi S, Korhonen P, Kanninen KM, Malm T, Koistinaho J, Auriola S, Fricker G, Puris E 2022. Increased Expression and Activity of Brain Cortical cPLA2 Due to Chronic Lipopolysaccharide Administration in Mouse Model of Familial Alzheimer's Disease. Pharmaceutics 14(11).
35. Taylor SC, Nadeau K, Abbasi M, Lachance C, Nguyen M, Fenrich J 2019. The Ultimate qPCR Experiment: Producing Publication Quality, Reproducible Data the First Time. Trends Biotechnol 37(7):761-774.
36. Uchida Y, Tachikawa M, Obuchi W, Hoshi Y, Tomioka Y, Ohtsuki S, Terasaki T 2013. A study protocol for quantitative targeted absolute proteomics (QTAP) by LC-MS/MS: application for inter-strain differences in protein expression levels of transporters, receptors, claudin-5, and marker proteins at the blood-brain barrier in ddY, FVB, and C57BL/6J mice. Fluids Barriers CNS 10(1):21.
37. Gynther M, Proietti Silvestri I, Hansen JC, Hansen KB, Malm T, Ishchenko Y, Larsen Y, Han L, Kayser S, Auriola S, Petsalo A, Nielsen B, Pickering DS, Bunch L 2017. Augmentation of Anticancer Drug Efficacy in Murine Hepatocellular Carcinoma Cells by a Peripherally Acting Competitive N-Methyl-d-aspartate (NMDA) Receptor Antagonist. J Med Chem 60(23):9885-9904.
38. Puris E, Auriola S, Korhonen P, Loppi S, Kanninen KM, Malm T, Koistinaho J, Gynther M 2021. Systemic Inflammation Induced Changes in Protein Expression of ABC Transporters and Ionotropic Glutamate Receptor Subunit 1 in the Cerebral Cortex of Familial Alzheimer`s Disease Mouse Model. J Pharm Sci.
39. Sjostedt N, Holvikari K, Tammela P, Kidron H 2017. Inhibition of Breast Cancer Resistance Protein and Multidrug Resistance Associated Protein 2 by Natural Compounds and Their Derivatives. Mol Pharm 14(1):135-146.
40. Sjostedt N, van den Heuvel J, Koenderink JB, Kidron H 2017. Transmembrane Domain Single-Nucleotide Polymorphisms Impair Expression and Transport Activity of ABC Transporter ABCG2. Pharm Res 34(8):1626-1636.
41. Burguin A, Diorio C, Durocher F 2021. Breast Cancer Treatments: Updates and New Challenges. J Pers Med 11(8).
42. Manjunath M, Choudhary B 2021. Triple-negative breast cancer: A run-through of features, classification and current therapies. Oncol Lett 22(1):512.
43. Nedeljkovic M, Tanic N, Prvanovic M, Milovanovic Z, Tanic N 2021. Friend or foe: ABCG2, ABCC1 and ABCB1 expression in triple-negative breast cancer. Breast Cancer 28(3):727-736.
44. Munoz-Sanchez J, Chanez-Cardenas ME 2019. The use of cobalt chloride as a chemical hypoxia model. J Appl Toxicol 39(4):556-570.
45. D'Ignazio L, Rocha S 2016. Hypoxia Induced NF-kappaB. Cells 5(1).
46. Bos R, Zhong H, Hanrahan CF, Mommers EC, Semenza GL, Pinedo HM, Abeloff MD, Simons JW, van Diest PJ, van der Wall E 2001. Levels of hypoxia-inducible factor-1 alpha during breast carcinogenesis. J Natl Cancer Inst 93(4):309-314.
47. Dales JP, Garcia S, Meunier-Carpentier S, Andrac-Meyer L, Haddad O, Lavaut MN, Allasia C, Bonnier P, Charpin C 2005. Overexpression of hypoxia-inducible factor HIF-1alpha predicts

early relapse in breast cancer: retrospective study in a series of 745 patients. Int J Cancer 116(5):734-739.
48. Linderholm BK, Hellborg H, Johansson U, Elmberger G, Skoog L, Lehtio J, Lewensohn R 2009. Significantly higher levels of vascular endothelial growth factor (VEGF) and shorter survival times for patients with primary operable triple-negative breast cancer. Ann Oncol 20(10):1639-1646.
49. Shibata A, Nagaya T, Imai T, Funahashi H, Nakao A, Seo H 2002. Inhibition of NF-kappaB activity decreases the VEGF mRNA expression in MDA-MB-231 breast cancer cells. Breast Cancer Res Treat 73(3):237-243.
50. Kort A, Durmus S, Sparidans RW, Wagenaar E, Beijnen JH, Schinkel AH 2015. Brain and Testis Accumulation of Regorafenib is Restricted by Breast Cancer Resistance Protein (BCRP/ABCG2) and P-glycoprotein (P-GP/ABCB1). Pharm Res 32(7):2205-2216.
51. Deng F, Sjostedt N, Santo M, Neuvonen M, Niemi M, Kidron H 2023. Novel inhibitors of breast cancer resistance protein (BCRP, ABCG2) among marketed drugs. Eur J Pharm Sci 181:106362.
52. Liang Y, Zheng T, Song R, Wang J, Yin D, Wang L, Liu H, Tian L, Fang X, Meng X, Jiang H, Liu J, Liu L 2013. Hypoxia-mediated sorafenib resistance can be overcome by EF24 through Von Hippel-Lindau tumor suppressor-dependent HIF-1alpha inhibition in hepatocellular carcinoma. Hepatology 57(5):1847-1857.

Acknowledgments

We would like to thank Ms. Julia Braun, Ms. Maret Fritzenschaft, Mr. Sebastian Buddecke and Ms. Maria del Pilar Palacios Cisneros are acknowledged for their excellent technical assistance. The UEF School of Pharmacy laboratory is supported by Biocenter Finland and Biocenter Kuopio.

Declaration of Competing Interest

The authors declare no conflict of interest. The funders had no role in the design of the study; in the collection, analyses, or interpretation of data; in the writing of the manuscript, or in the decision to publish the results.

Data Availability Statement

The data presented in this study are available upon request from the corresponding author.

Figure legends

Fig. 1. A) $CoCl_2$ toxicity in MDA-MB-231 cells after 72 h. B) The mRNA expression of HIF1 in MDA-MB-231 cells in normoxia, $CoCl_2$ induced pseudohypoxia without and with 0.5 µM JJKK048 treatment. The data are presented as mean ± SD, (n=3). The HIF1 to GAPDH protein expression ratio analyzed by Western blot in MDA-MB-231 cells in normoxia, $CoCl_2$ induced pseudohypoxia without and with 0.5 µM JJKK048 treatment. Statistical significance of differences between the groups was evaluated by One-way ANOVA followed by Tukey's multiple comparisons test. Data is represented as mean ± SD, (n=4). **P* < 0.05; ***P* < 0.01.

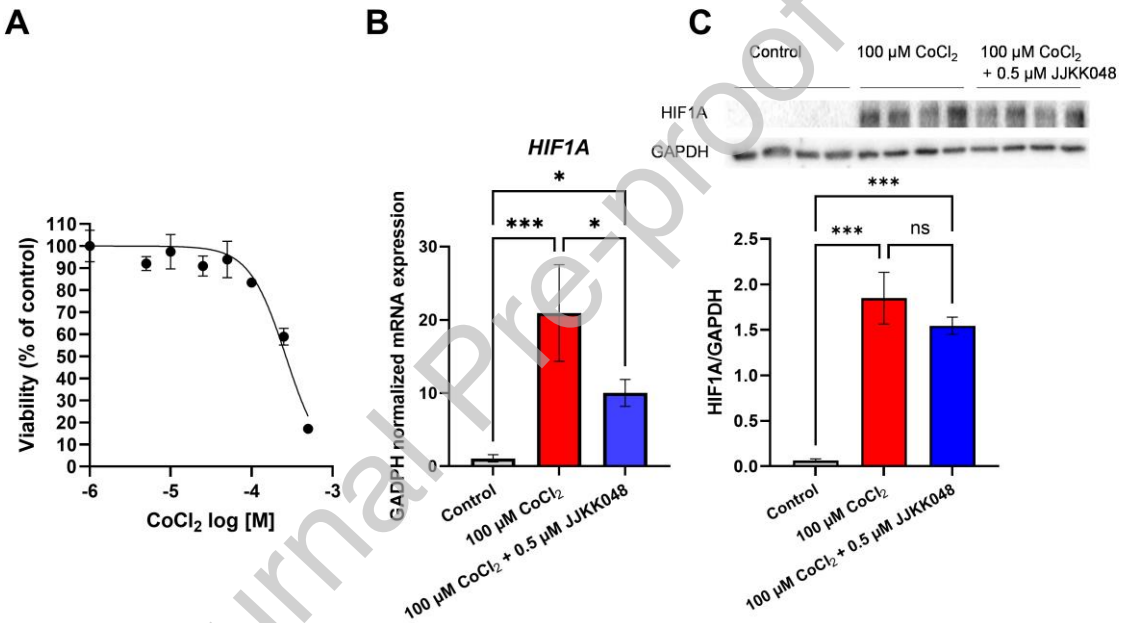

Fig. 2. A) Phosphorylated / total NFκB p65 expression in MDA-MB-231 cells in normoxia, $CoCl_2$ induced pseudohypoxia without and with 0.5 μM JJKK048 treatment. Statistical significance of differences between the groups was evaluated by One-way ANOVA followed by Tukey's multiple comparisons test. Data is represented as mean ± SD. ***P* < 0.01; ****P* < 0.001; *****P* < 0.0001. B) The mRNA expression of NFκB signaling inducible genes in MDA-MB-231 cells in normoxia, $CoCl_2$ induced pseudohypoxia without and with 0.5 μM JJKK048 treatment. Statistical significance of differences between the groups was evaluated by One-way ANOVA followed by Tukey's multiple comparisons test. Data is represented as mean ± SD, (n=4). **P* < 0.05; ***P* < 0.01.

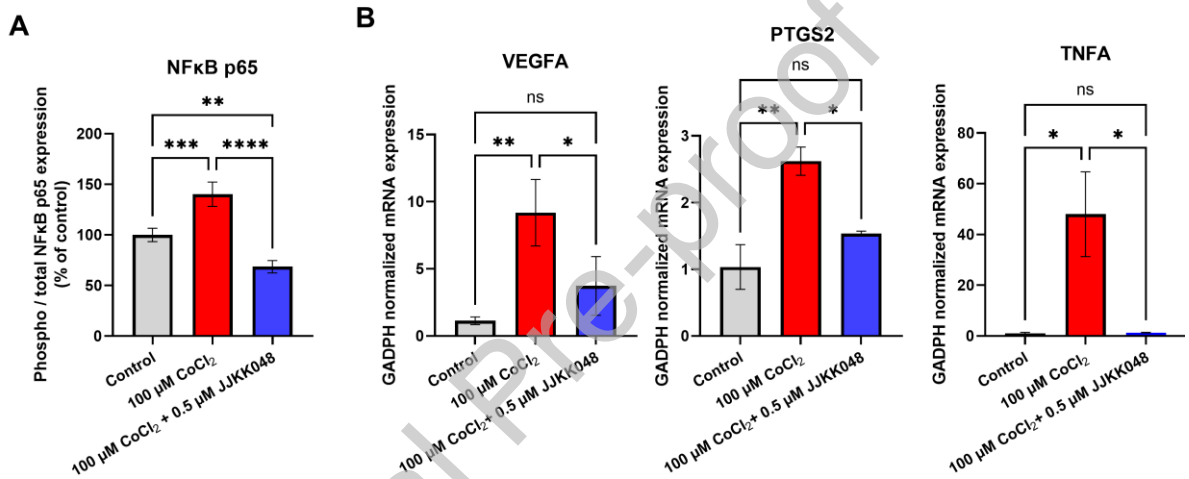

Fig. 3. A) MAGL protein expression in MDA-MB-231 cells in normoxia, $CoCl_2$ induced pseudohypoxia without and with 0.5 µM JJKK048 treatment. B) JJKK048 toxicity in MDA-MB-231 cells in normoxia (black circles) and $CoCl_2$ induced pseudohypoxia (red triangles). C) JJKK048 cell accumulation in normoxia and $CoCl_2$ induced pseudohypoxia. Statistical significance of differences between the groups in A was evaluated by One-way ANOVA followed by Tukey's multiple comparisons test. The statistical significance of differences between the groups in C was evaluated by t-test. Data are represented as mean ± SD, (n=3). *$P < 0.05$.

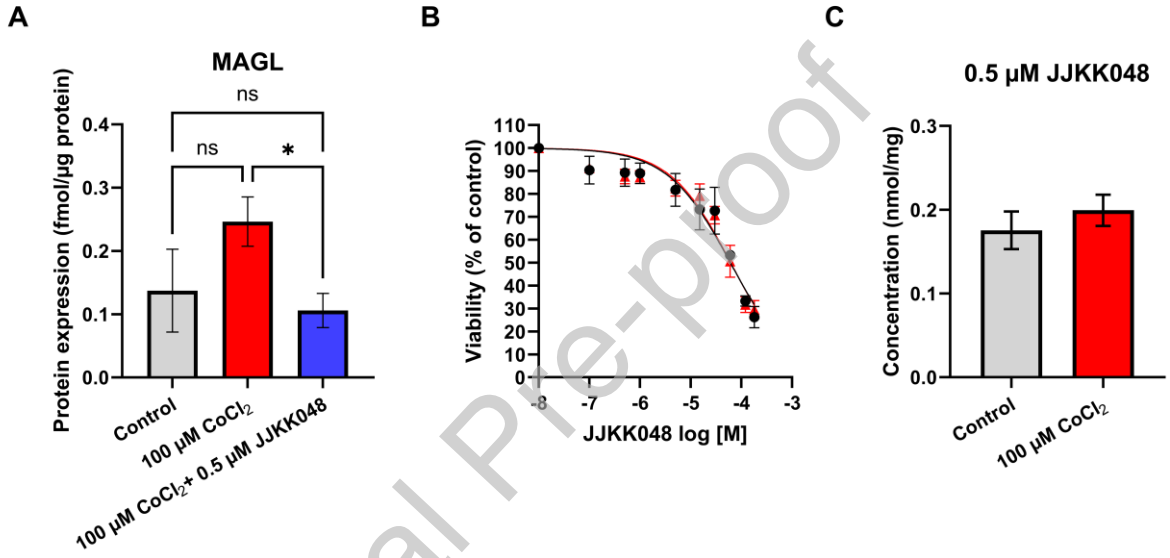

Fig. 4. A) ABCG2/BCRP gene and protein expression in MDA-MB-231 cells in normoxia, $CoCl_2$ induced pseudohypoxia without and with JJKK048 treatment. Statistical significance of differences between the groups was evaluated by One-way ANOVA followed by Tukey's multiple comparisons test. Data is represented as mean ± SD, (n=3). **P* < 0.05; ***P* < 0.01; *****P* < 0.0001. B) Lucifer yellow and regorafenib cell accumulation in MDA-MB-231 cells in normoxia, $CoCl_2$ induced pseudohypoxia without and with JJKK048, and in $CoCl_2$ induced pseudohypoxia co-incubated with 1 µM Ko143. Statistical significance of differences between the groups was evaluated by One-way ANOVA followed by Tukey's multiple comparisons test. Data is represented as mean ± SD, (n=4). **P* < 0.05; ***P* < 0.01; ****P* < 0.001; *****P* < 0.0001.

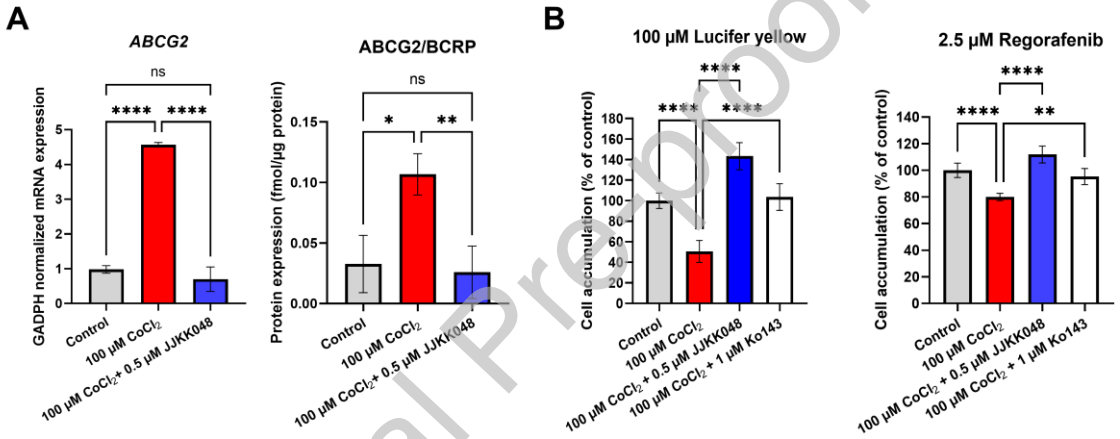

Fig 5. Uptake of 100 µM lucifer yellow and 0.5 µM regorafenib with and without 1 µM Ko143 in human ABCG2 expressing vesicles. The statistical significance of differences between the groups was evaluated by unpaired t-test. Data is represented as mean ± SD, (n=3). ***P* < 0.01; *****P* < 0.0001.

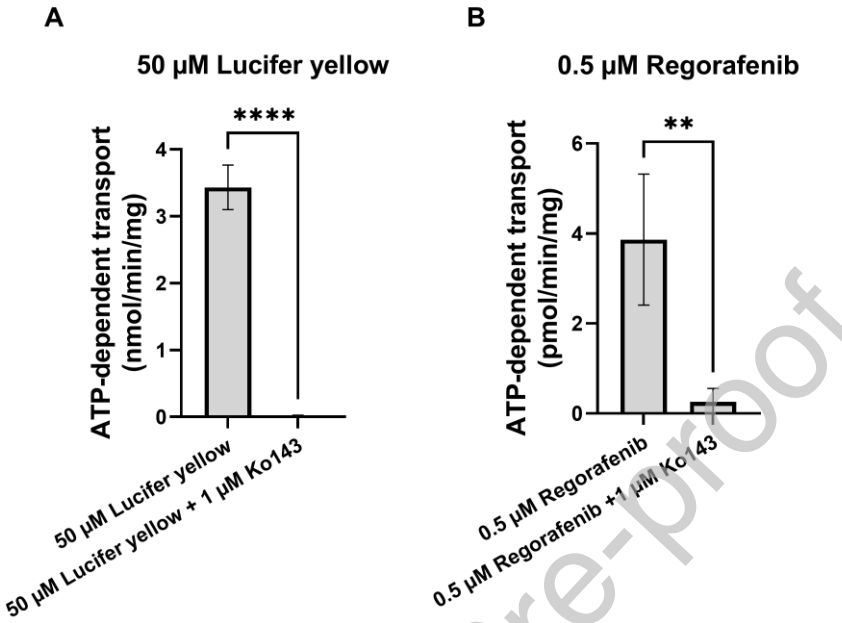

Fig. 6. A) Regorafenib effect on MDA-MB-231 cell invasiveness in normoxia, $CoCl_2$ induced pseudohypoxia without and with JJKK048 after 24 h incubation. The data are presented as mean ± SD, (n=3). Statistical significance of changes between the groups was evaluated by One-way ANOVA followed by Tukey's multiple comparisons test. B) Regorafenib effect on MDA-MB-231 cell viability in normoxia, $CoCl_2$ induced pseudohypoxia without and with JJKK048. The IC_{50} values are presented as mean ± SD, (n=3). Statistical significance of changes between the groups was evaluated by One-way ANOVA followed by Tukey's multiple comparisons test. **P* < 0.05 compared to control; $^{\#\#}P$ < 0.01 compared to 100 µM $CoCl_2$.

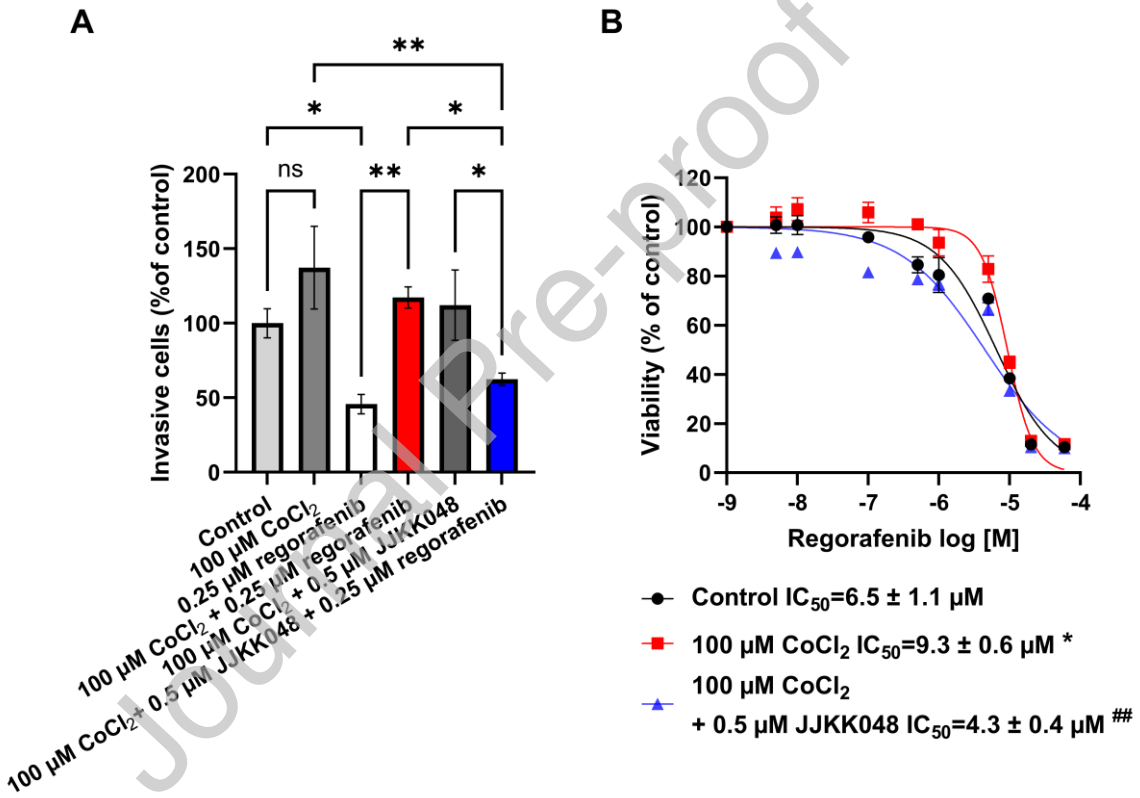

Tables

Table 1. Sequences of qRT-PCR primers.

Gene	Forward Primer	Reverse Primer
GADPH	5′-CCATCACCATCTTCCAGGAGCGA -3′	5′-GGATGACCTTGCCCACAGCCTTG-3′
ABCG2	5′-TATAGCTCAGATCATTGTCACAGTC-3′	5′-GTTGGTCGTCAGGAAGAAGA-3′
ABCB1	5′-TGCTCAGACAGGATGTGAGTT-3′	5′-AATTACAGCAAGCCTGGAAC-3′
HIF1A	5′-CATAAAGTCTGCAACATGGAAGGT-3′	5′-ATTTGATGGGTGAGGAATGGGTT-3′
VEGFA	5′-ATCTTCAAGCCATCCTGTGTGC-3′	5′-CAAGGCCCACAGGGATTTTC-3′
PTGS2	5′-GAATGGGGTGATGAGCAGTT-3′	5′-CAGAAGGGCAGGATACAGC-3′
TNFA	5′-CTTCTGCCTGCTG CACTTTGGA-3′	5′-TCCCAAAGTAGACCTGCCCAGA-3′

Table 2. Amino acid sequences of probe peptides, retention time and MRM transitions for the LC-MS/MS analysis of target proteins.

Protein	St/IS	Unique amino acid sequence	Retention time (min)	MRM transitions (m/z)				
				Q1	Q3.1	Q3.2	Q3.3	Q3.4
MAGL	St	LTVPFLLLQGSADR	32.1	765.4	1216.7	746.4	505.2	
	IS	LTVPFLLLQGSAD**R***	32.1	770.4	1226.7	756.4	515.2	
ABCB1	St	NTTGALTTR	8.7	467.7	719.4	618.3	561.3	490.2
	IS	NTTGALTT**R***	8.7	472.7	729.4	628.3	517.3	500.3
ABCG2	St	SSLLDVLAAR	27.5	522.8	757.4	644.3	529.3	
	IS	SSLLDVLAA**R***	27.5	527.8	767.4	654.3	539.3	
Na^+/K^+–ATPase	St	AAVPDAVGK	12.2	414.3	685.4	586.3	489.3	204.1
	IS	AAVPDAVG**K***	12.2	418.3	693.4	594.3	497.3	212.1

St – standard, IS – internal standard.
Bold letter with* denotes labeled arginine (R) or lysine (K) with a stable isotope ^{13}C and ^{15}N.

Graphical abstract